

AePW-4 High-Angle Working Group Meeting



July 11, 2024

Pawel Chwalowski

Pawel.Chwalowski@nasa.gov

Agenda July 11



- BSCW experimental data review, Pawel Chwalowski
- BSCW Reduced-order model flutter results, Walt Silva
- August 8, BSCW ROM results, Michael Candon, Royal Melbourne Institute of Technology, RMIT University.
- August 8, BSCW FUN3D DDES, Pawel Chwalowski

Schedule/Timeline/Logistics



- Monthly meetings on second Thursday of each month at 10 am EDT
 - IFASD 2024: 17 – 21 June 2024, The Hague - Bret Stanford
 - AIAA Aviation 2024: Las Vegas, NV - Bret Stanford
 - AIAA SciTech 2025: Orlando, FL (?)
 - Spring 2025: New BSCW Experiment (Data release ?)
 -
 - AIAA Aviation 2026: DPW-8 and AePW-4 Workshop
-
- Call for papers for Australian International Aerospace Congress: Professor Pier Marzocca, RMIT, pier.marzocca@rmit.edu.au

<https://www.engineersaustralia.org.au/learning-and-events/conferences-and-major-events/australian-international-aerospace-congress>

AePW-4 High-Angle WG Cases



- Mandatory
 - Flutter prediction at Mach 0.80 and angle-of-attack sweep: $0^{\circ} - 6^{\circ}$
- Optional
 - Flutter prediction at Mach 0.78, 0.76, 0.74 and angle-of-attack 3°

Past Experimental Data



EXPERIMENTAL UNSTEADY PRESSURES AT FLUTTER ON THE SUPERCRITICAL WING BENCHMARK MODEL

AIAA-93-1592-CP

Bryan E. Dansberry, Michael H. Durham*, Robert M. Bennett**, José A. Rivera*, Walter A. Silva*, and Carol D. Wieseman*; Structural Dynamics Division, NASA Langley Research Center, Hampton, VA 23681-0001 and David L. Turnock*
Lockheed Engineering and Sciences Corporation

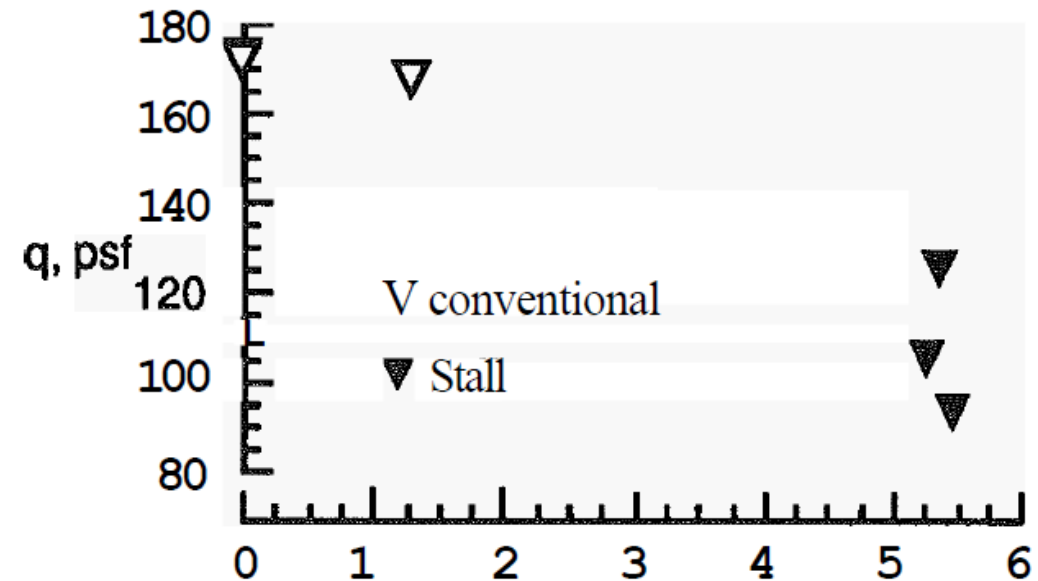
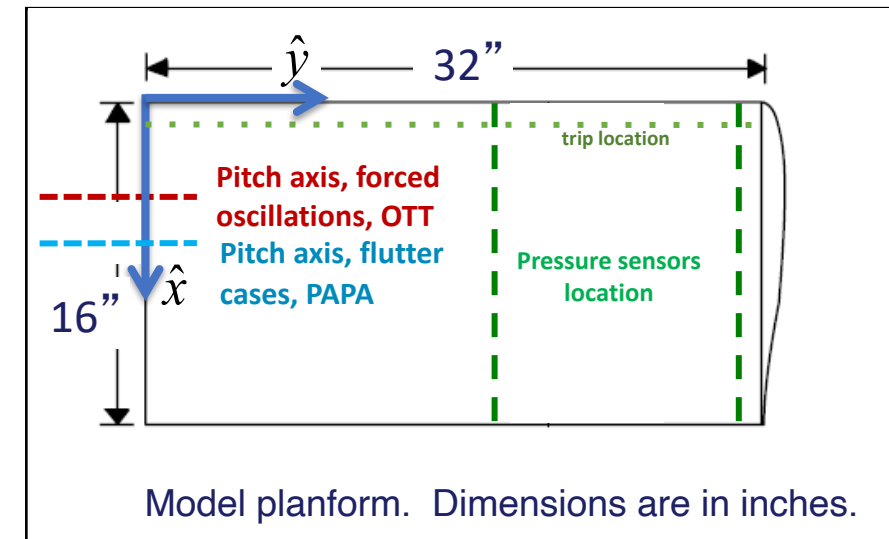
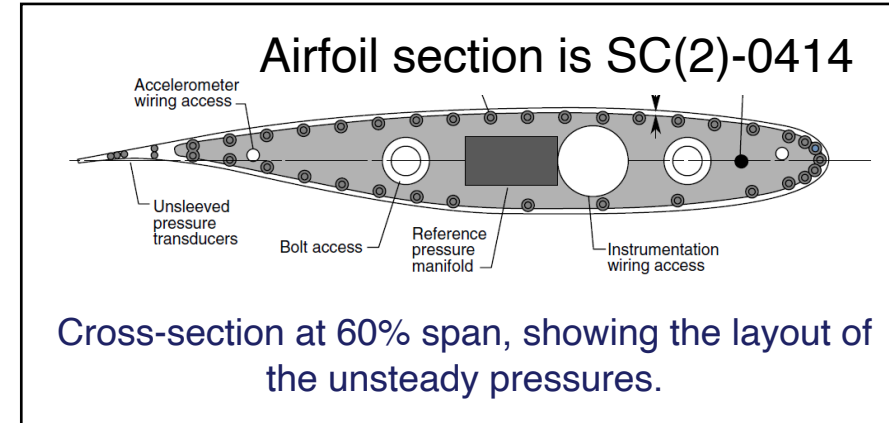
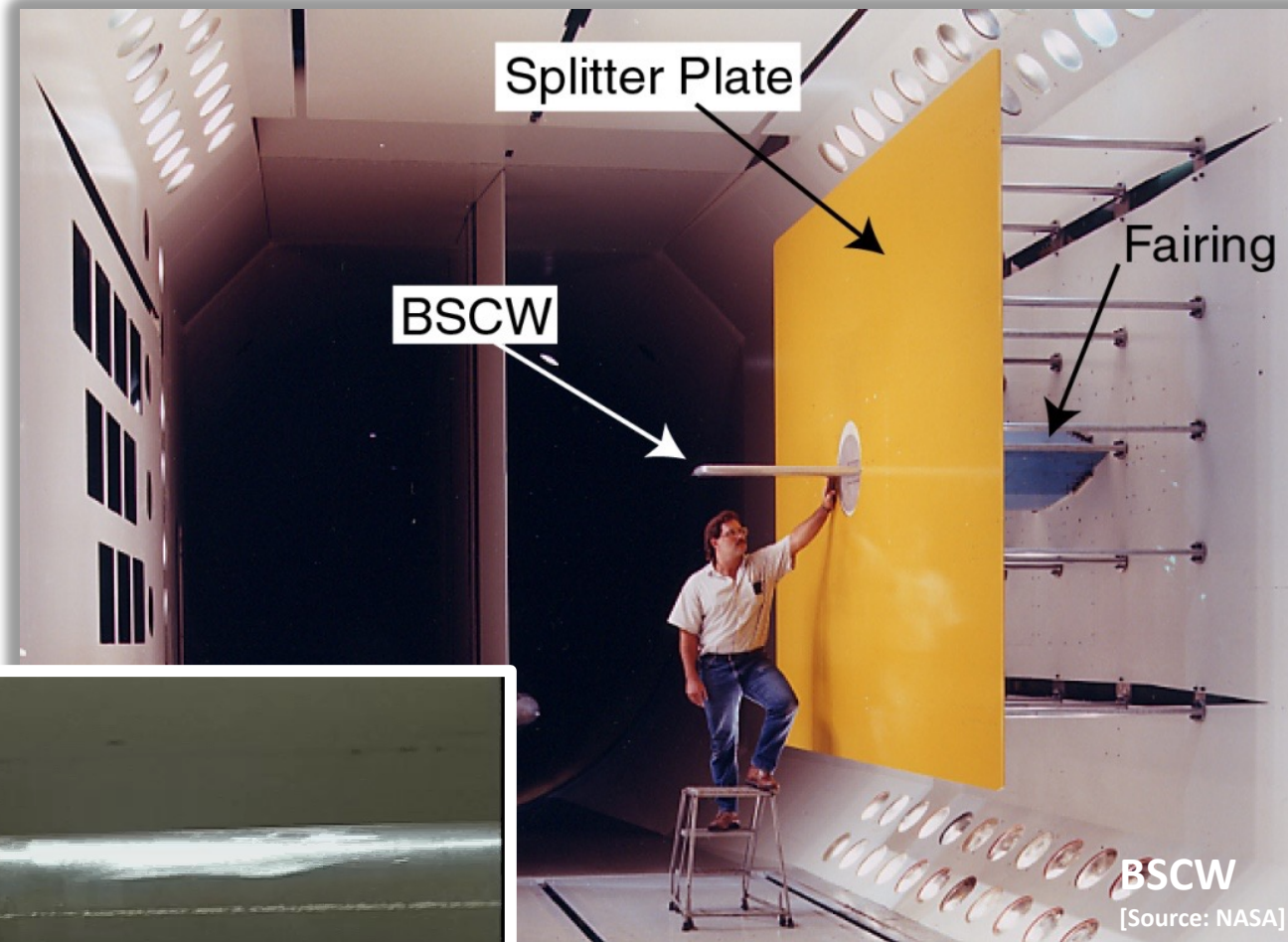


Figure 9. Stall flutter boundary in R-12 at $M = 0.80$.

High-Angle WG: BSCW Wing Configuration

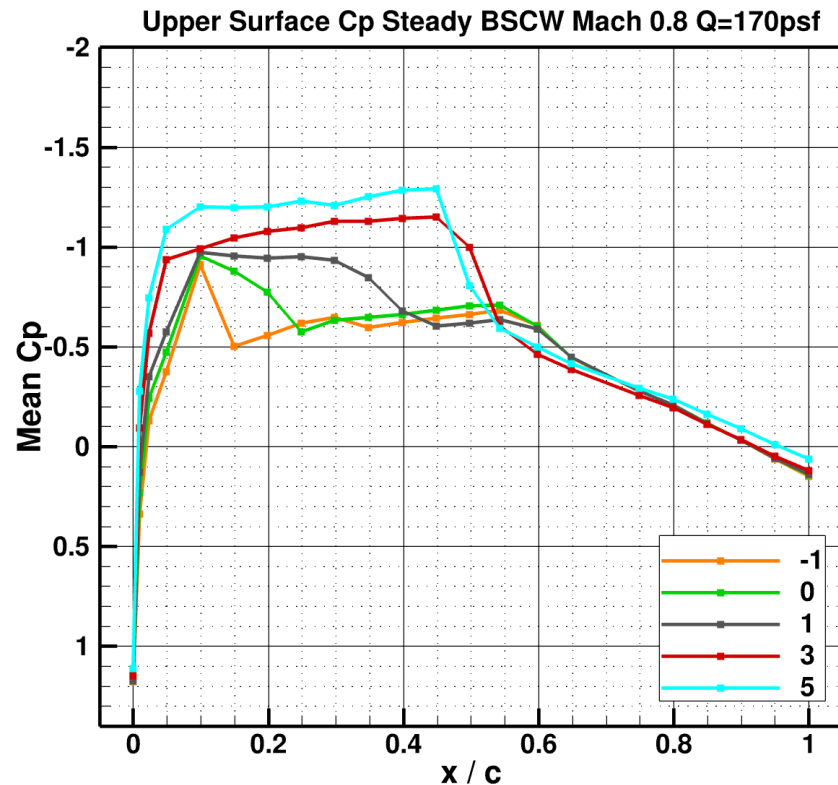


Rigidized OTT or PAPA: BSCW held at angle of attack

BSCW Experimental Data



Shock-Buffet Prediction Report in Support of the High Angle Working Group at the Third Aeroelastic Prediction Workshop
<https://doi.org/10.2514/6.2024-0417>, Figure 3b

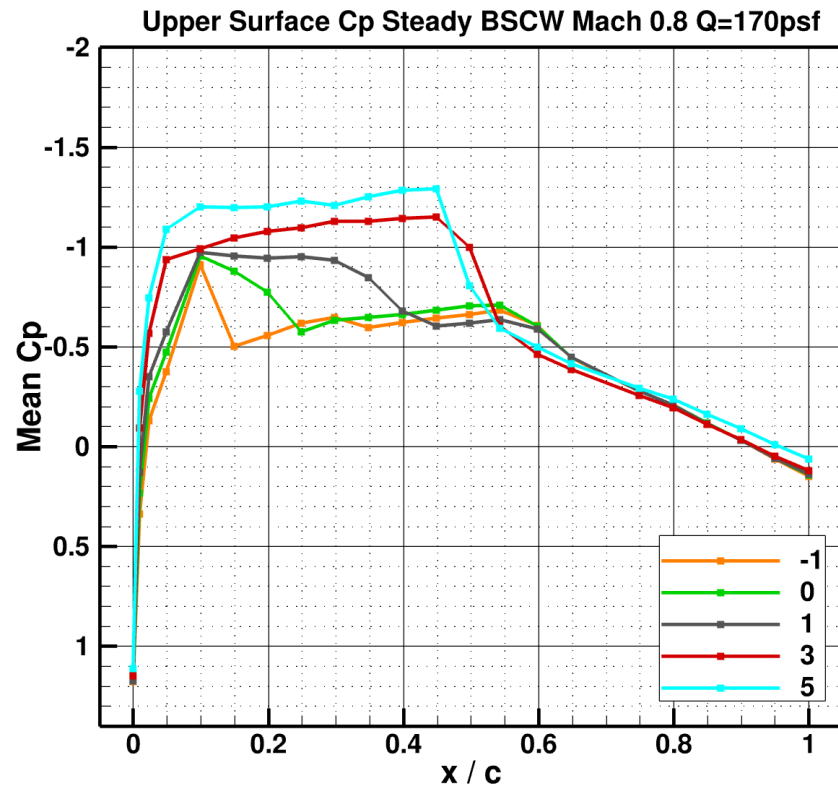


Rigidized OTT !!!

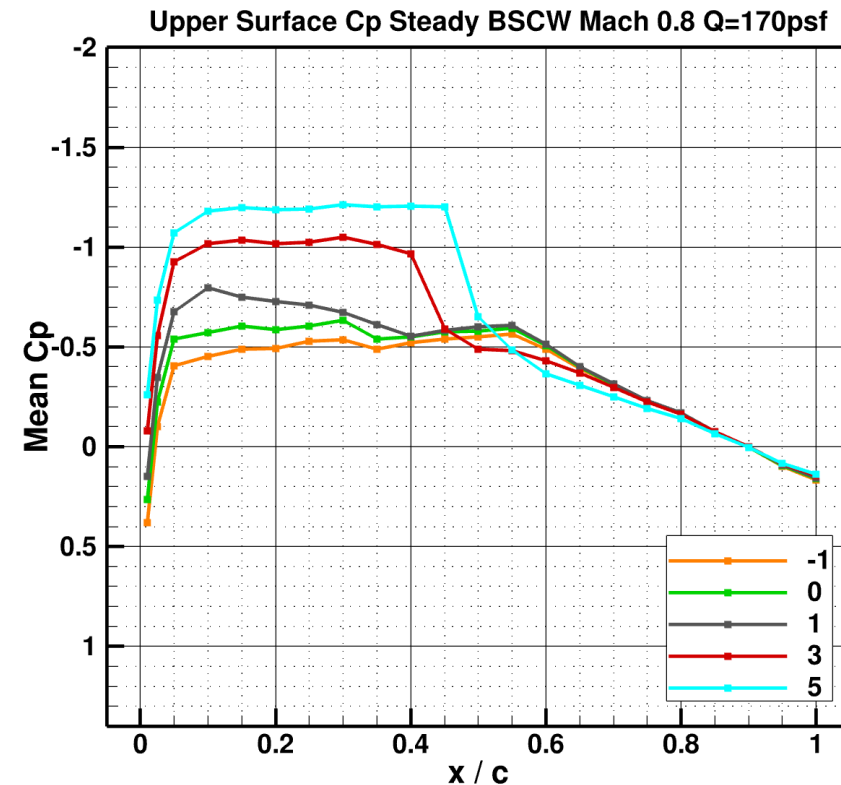
BSCW Experimental Data



Shock-Buffer Prediction Report in Support of the High Angle Working Group at the Third Aeroelastic Prediction Workshop
<https://doi.org/10.2514/6.2024-0417>, Figure 3b



Rigidized OTT !!!

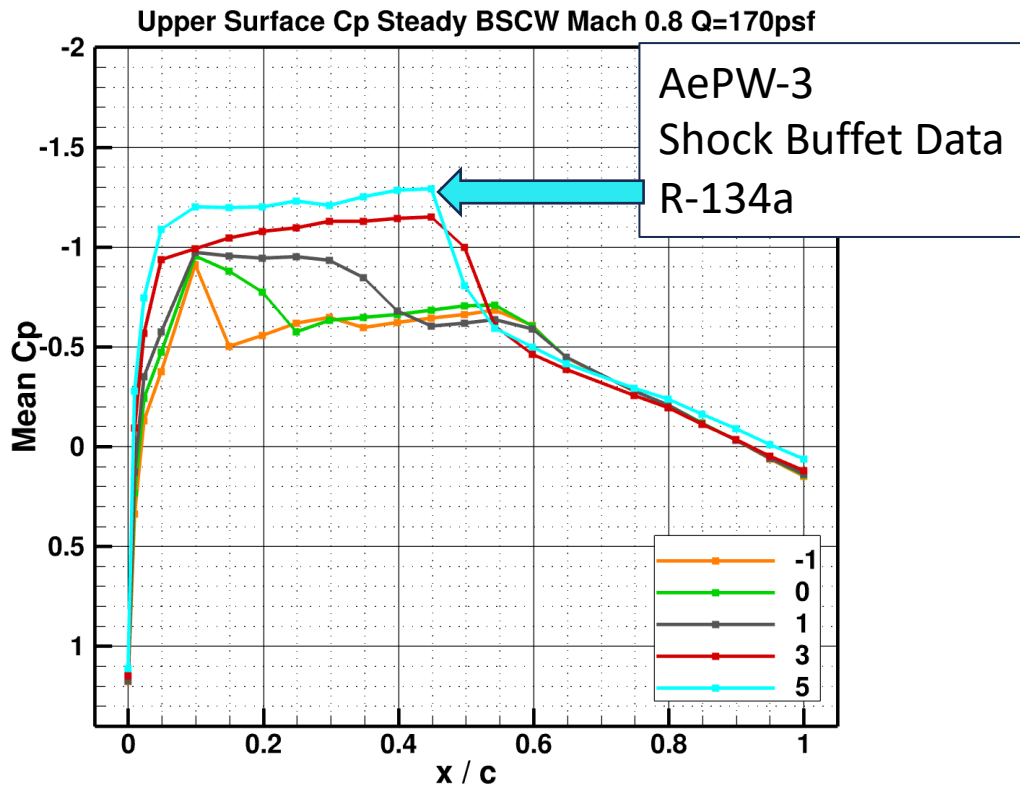


Rigidized PAPA !!!

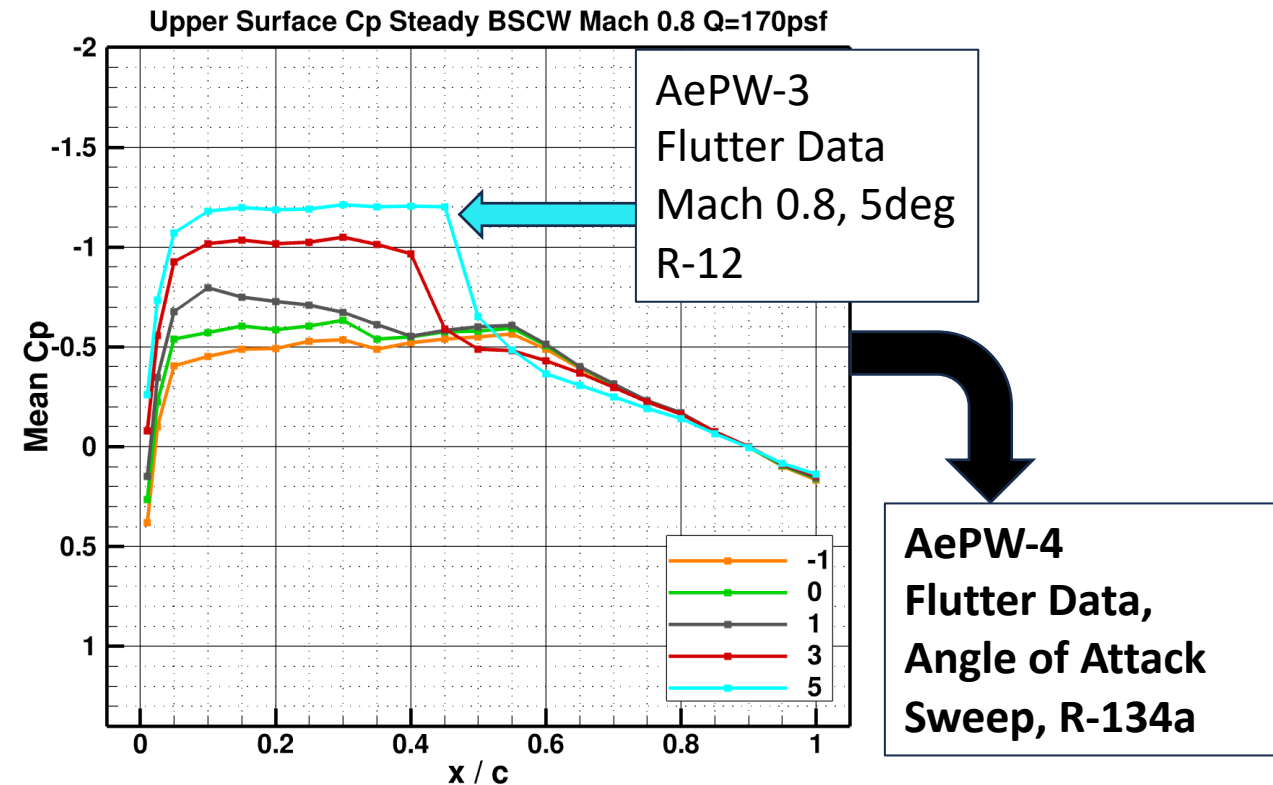
BSCW Experimental Data



Shock-Buffer Prediction Report in Support of the High Angle Working Group at the Third Aeroelastic Prediction Workshop
<https://doi.org/10.2514/6.2024-0417>, Figure 3b



Rigidized OTT !!!

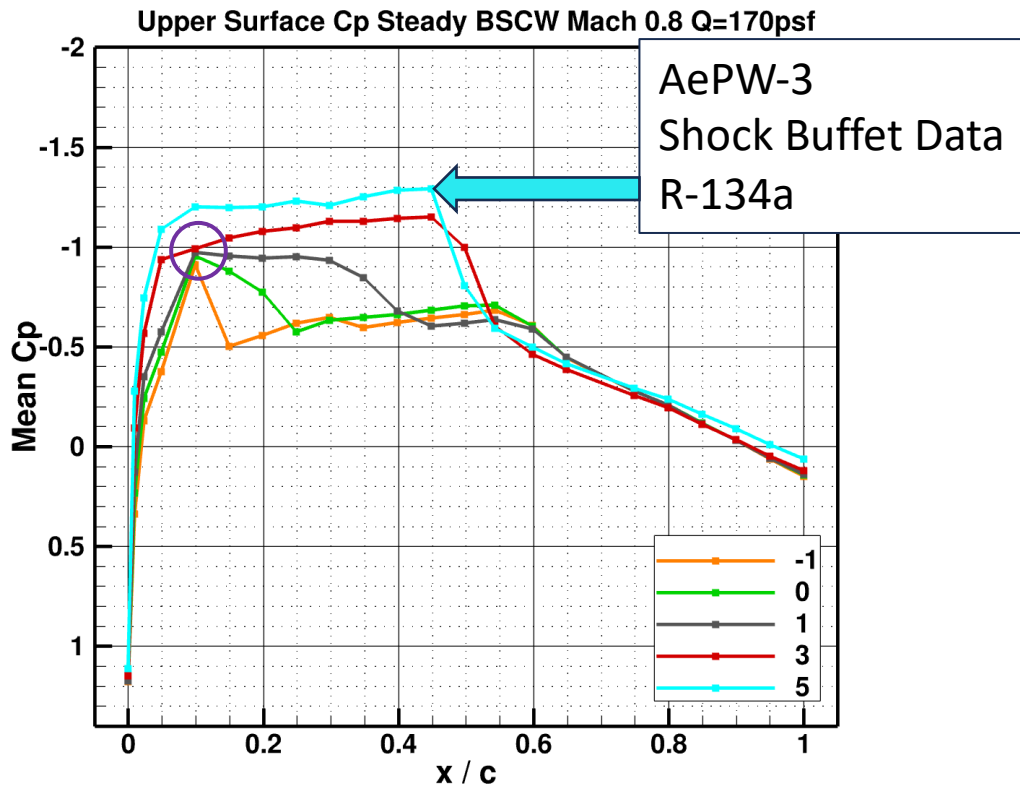


Rigidized PAPA !!!

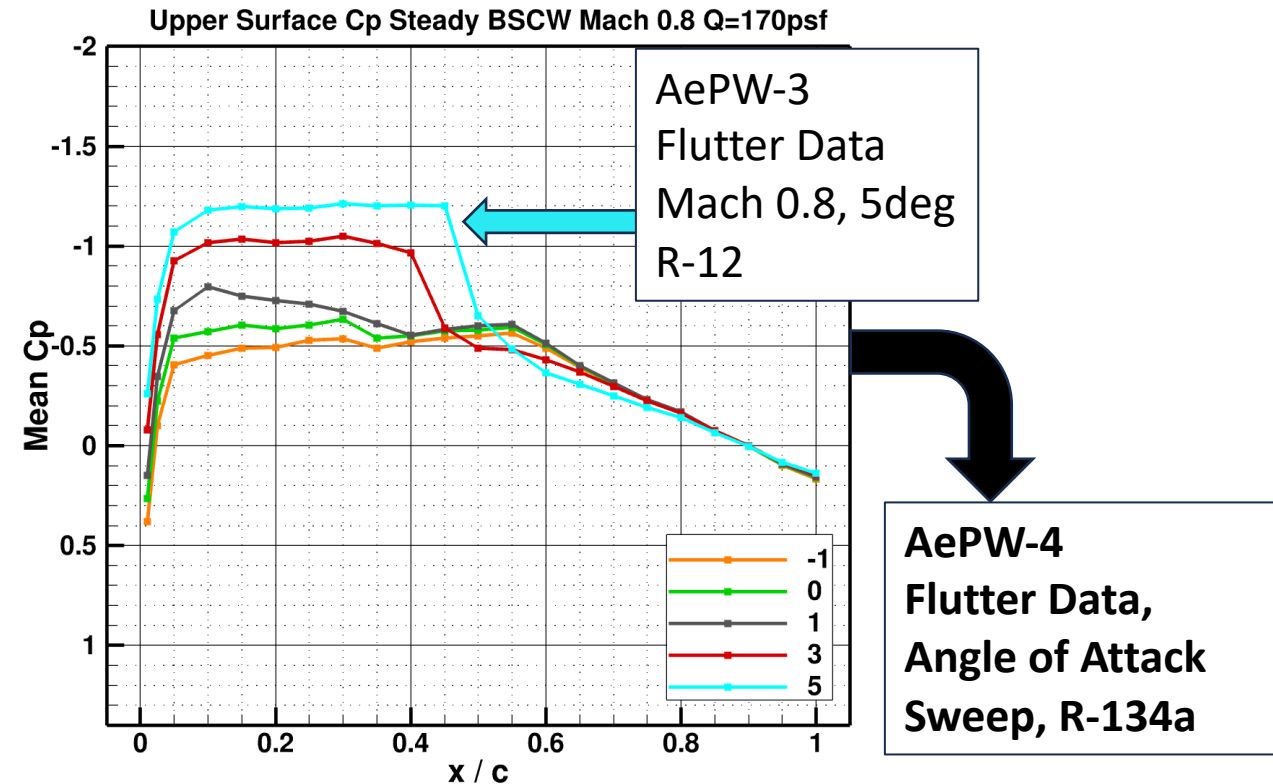
BSCW Experimental Data, Upper Surface



Shock-Buffer Prediction Report in Support of the
High Angle Working Group at the
Third Aeroelastic Prediction Workshop
<https://doi.org/10.2514/6.2024-0417>, Figure 3b



Rigidized OTT !!!



Rigidized PAPA !!!

Dansberry Paper, AIAA93-1592, BSCW PAPA flutter

In air the boundaries were defined with and without fixed boundary layer transition. To fix the transition point a grit strip, 0.25" in width, running from root to tip on both the upper **and** lower surfaces was used. Two fixed transition configurations and one free transition configuration were tested in air. In R-12 only one configuration was tested. It had fixed transition.

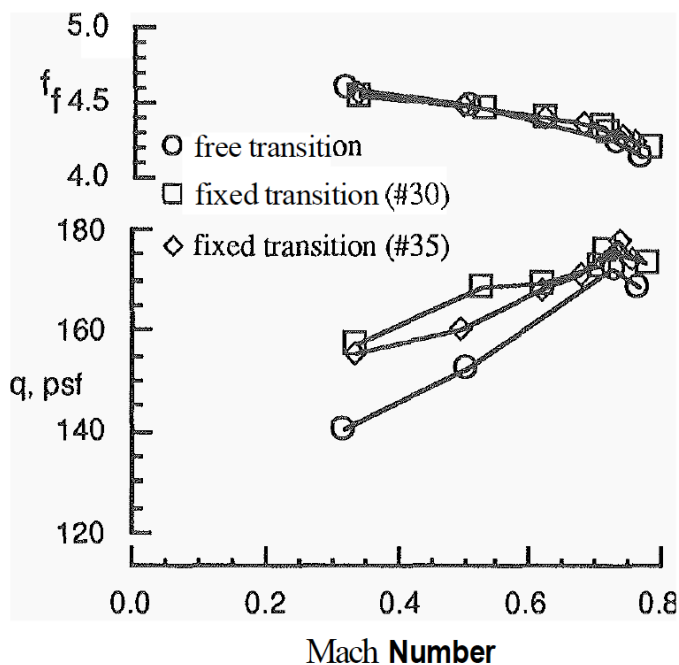


Figure 6. Transition effects on conventional flutter boundary in air ($\alpha_m=0^\circ$).

Figure 6 shows the effects on the flutter boundary in air of fixing the point on the model where the boundary layer transitions from laminar to turbulent. As mentioned previously, two different fixed transition configurations were tested. In both cases the transition point was fixed at 6.5 percent chord on both the upper and lower surfaces. The difference in the two configurations was a change in grit size from #30 to #35. Also, the transition strip used for the #35 grit configuration was wrapped around the tip while the #30 configuration left transition free on the tip. As can be seen in the figure, the main effect of fixing the transition point was to increase the flutter dynamic pressure. This effect is greater at subsonic Mach numbers than at transonic Mach numbers. The two transition fixed configurations show no significant differences.

All rigidized data were acquired using the #35 grit fixed transition configuration.

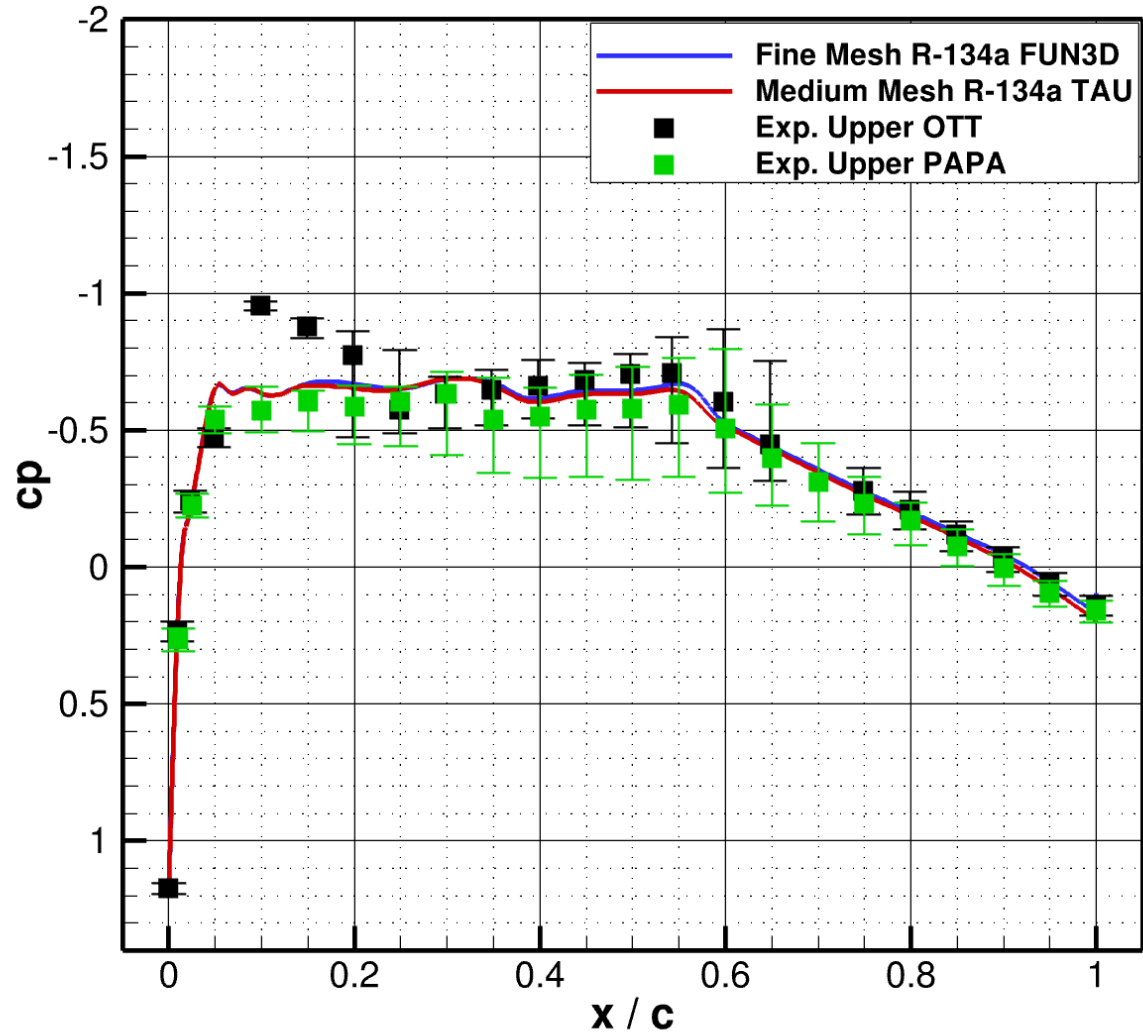
Piatak Paper, AIAA2002-0171: BSCW OTT

Boundary-layer transition was fixed at 7.5 percent chord using a #30 grit strip.

PAPA vs. OTT vs. TAU vs. FUN3D (steady)



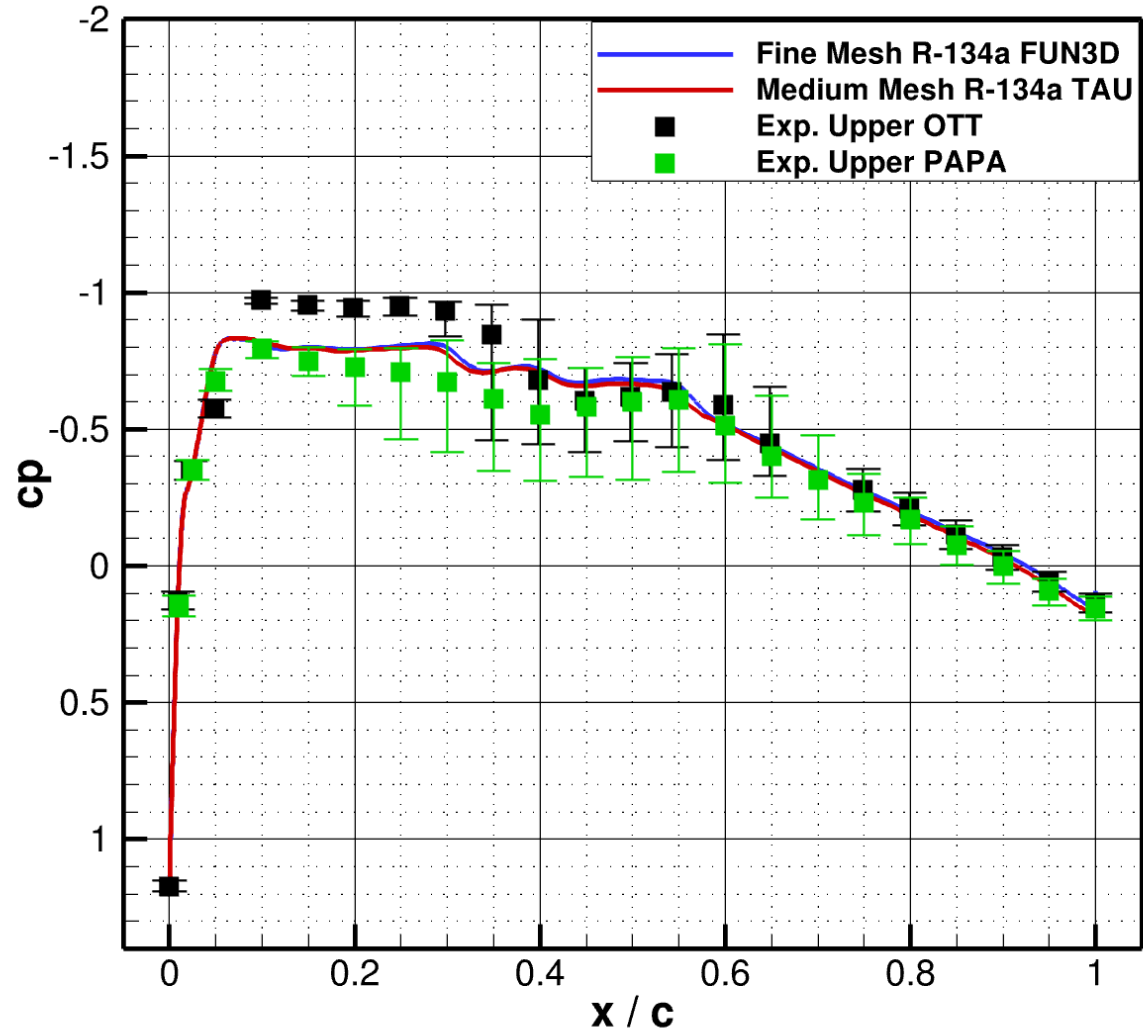
BSCW Mach = 0.8, AoA = 0 deg, Q = 169 psf
60% Span Station



PAPA vs. OTT vs. TAU vs. FUN3D (steady)



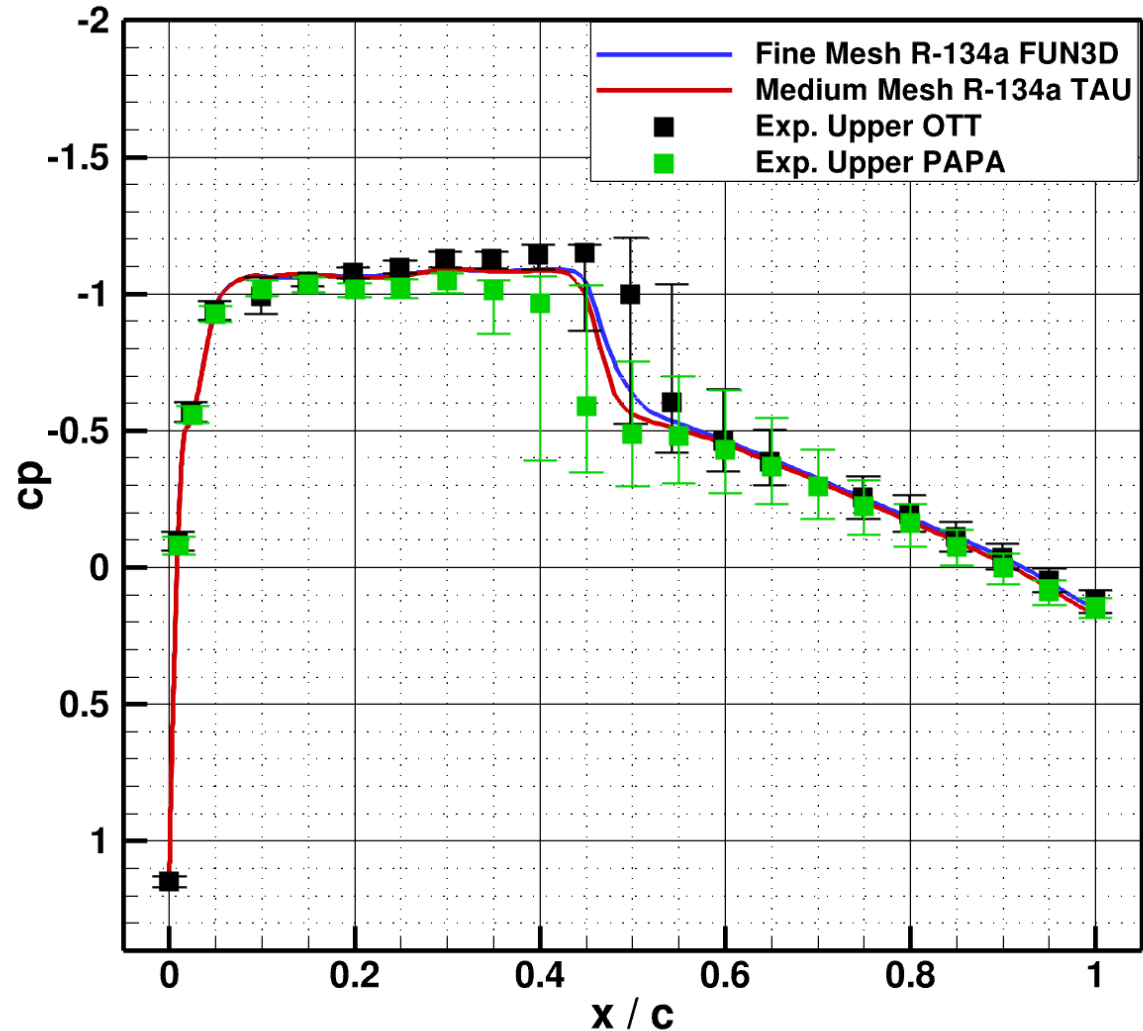
BSCW Mach = 0.8, AoA = 1 deg, Q = 169 psf
60% Span Station



PAPA vs. OTT vs. TAU vs. FUN3D (steady)



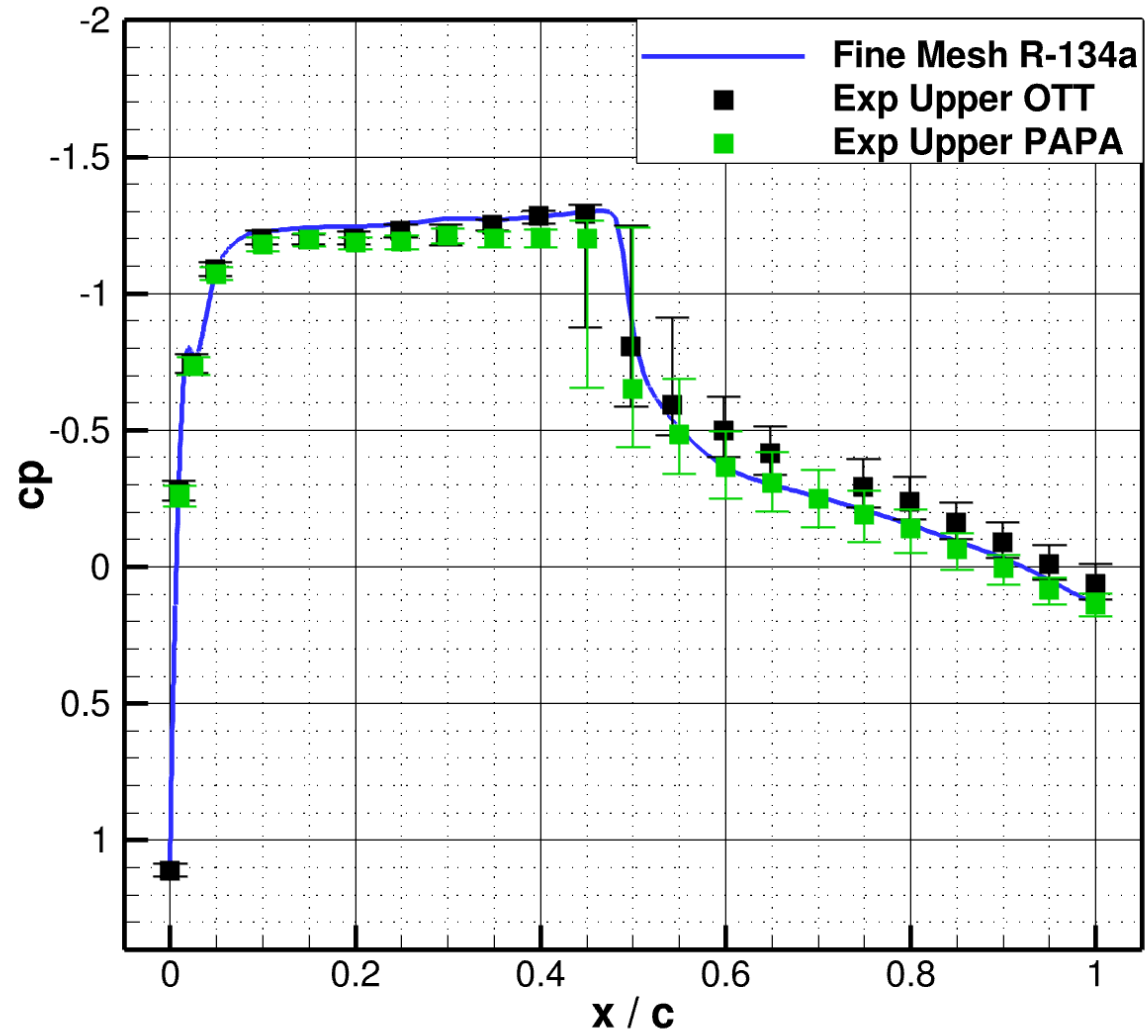
BSCW Mach = 0.8, AoA = 3 deg, Q = 169 psf
60% Span Station



PAPA vs. OTT vs. TAU vs. FUN3D (steady)



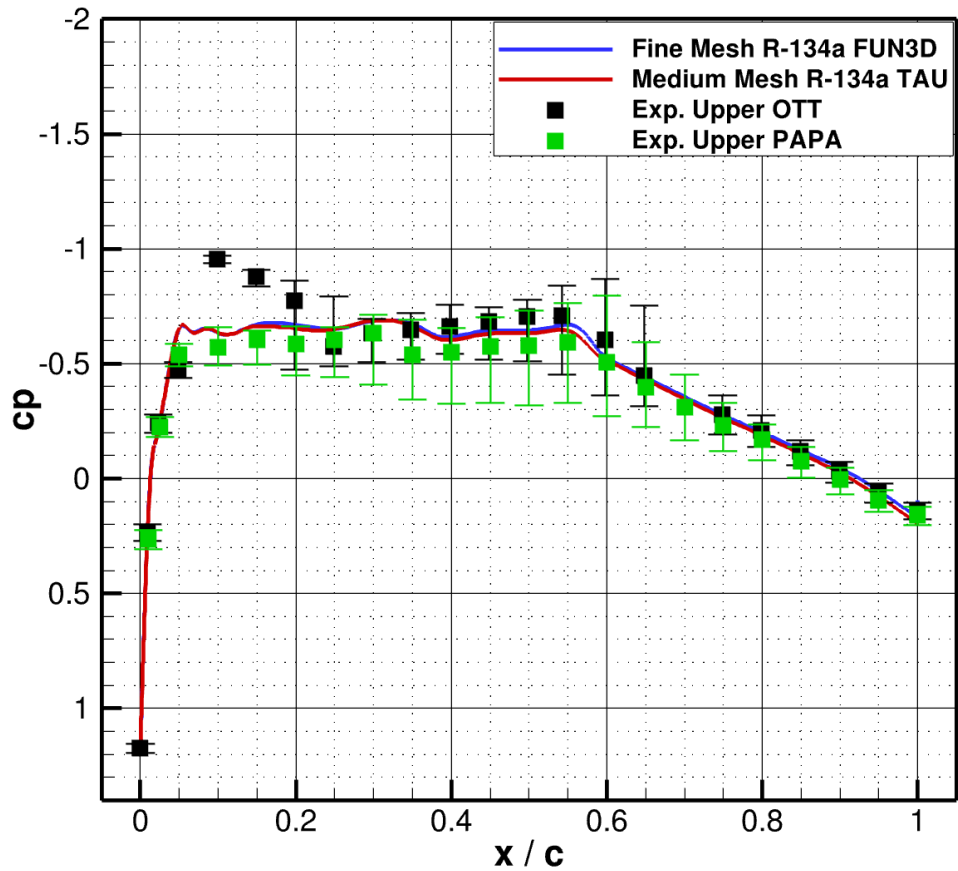
BSCW Mach = 0.8, AoA = 5 deg, Q = 169 psf
60% Span Station



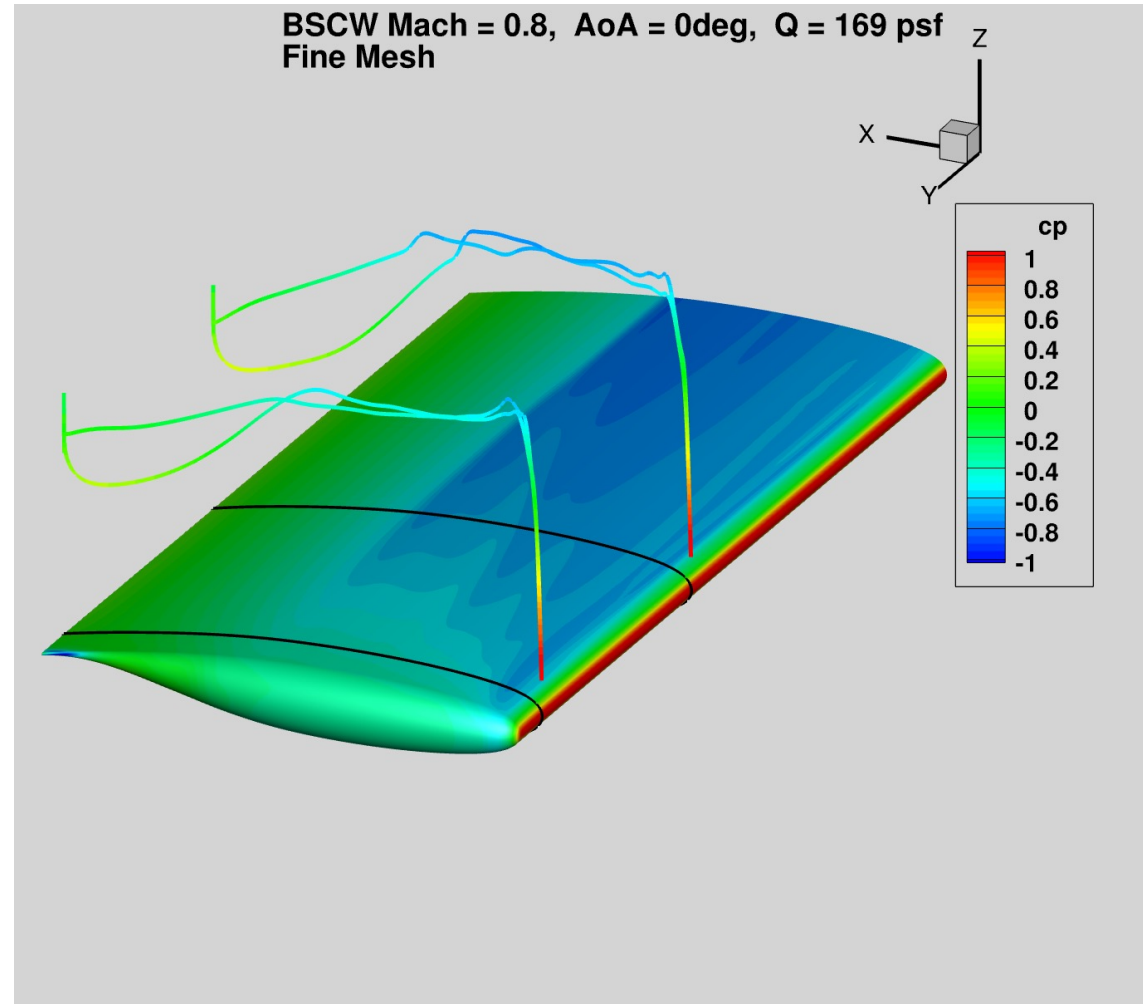
PAPA vs. OTT vs. TAU vs. FUN3D (steady)



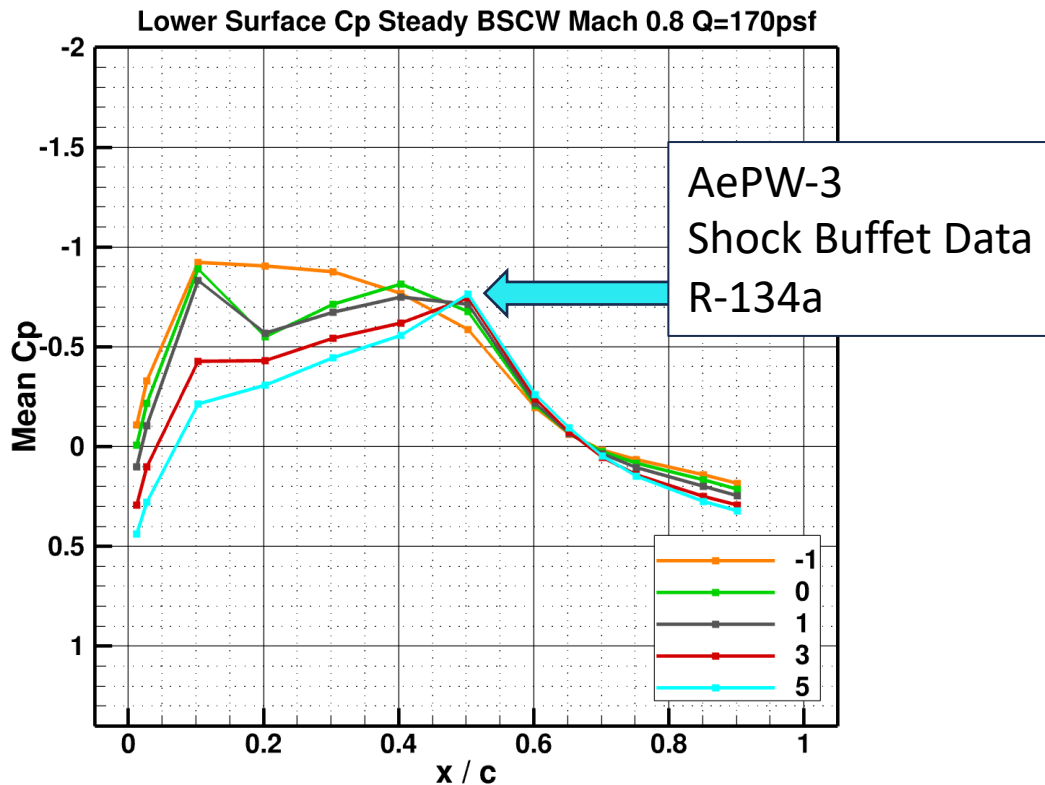
BSCW Mach = 0.8, AoA = 0 deg, Q = 169 psf
60% Span Station



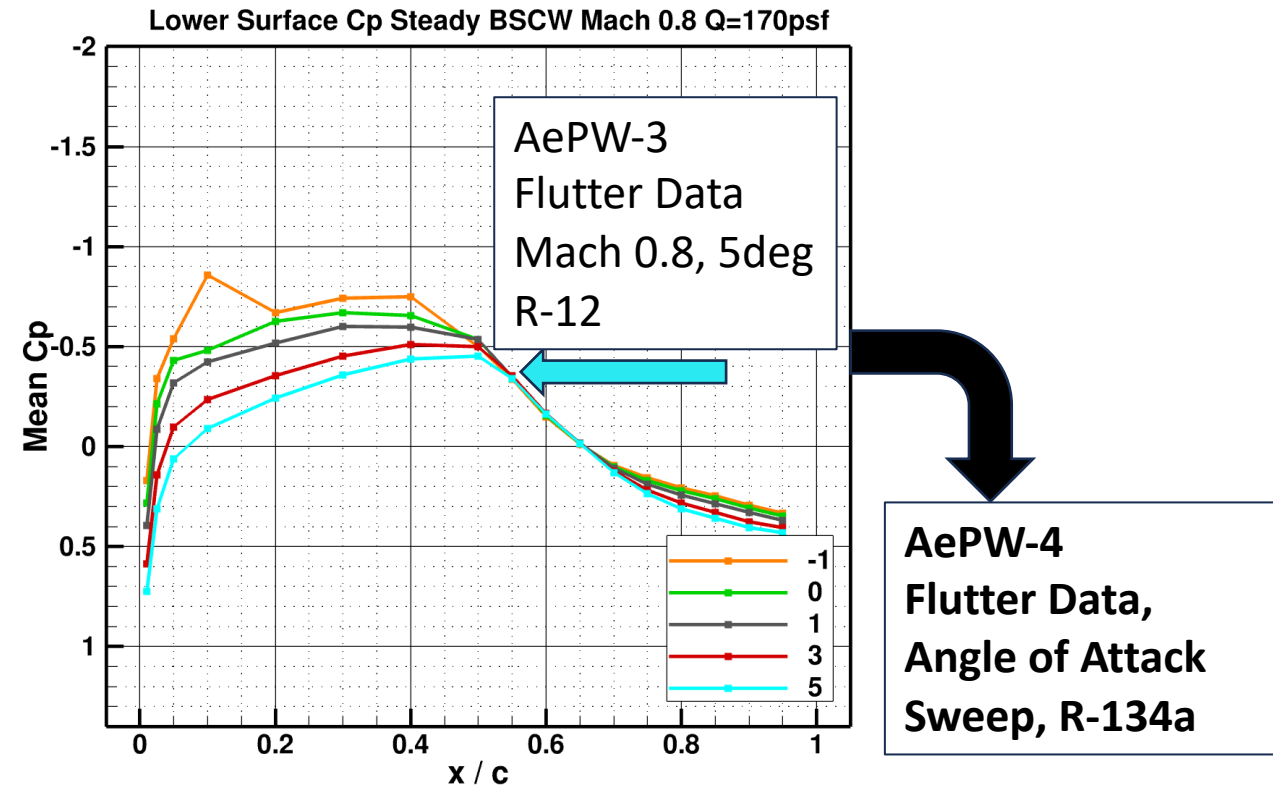
BSCW Mach = 0.8, AoA = 0deg, Q = 169 psf
Fine Mesh



BSCW Experimental Data, Lower Surface



Rigidized OTT !!!



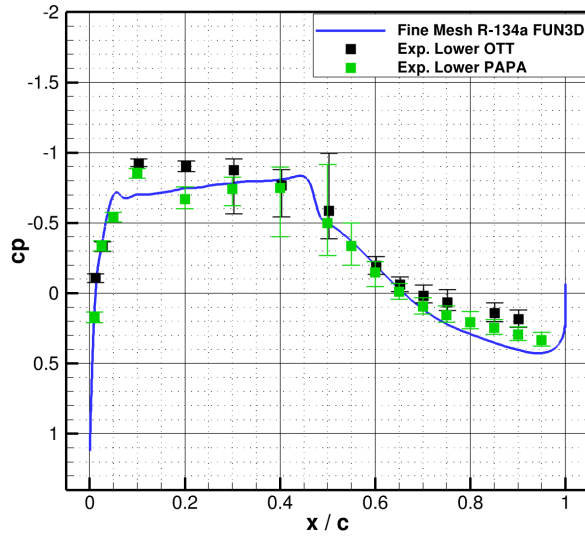
**AePW-4
Flutter Data,
Angle of Attack
Sweep, R-134a**

Rigidized PAPA !!!

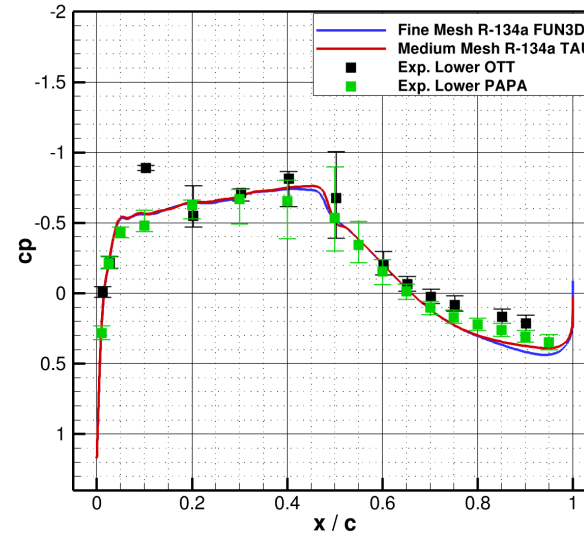
PAPA vs. OTT vs. TAU vs. FUN3D (steady)



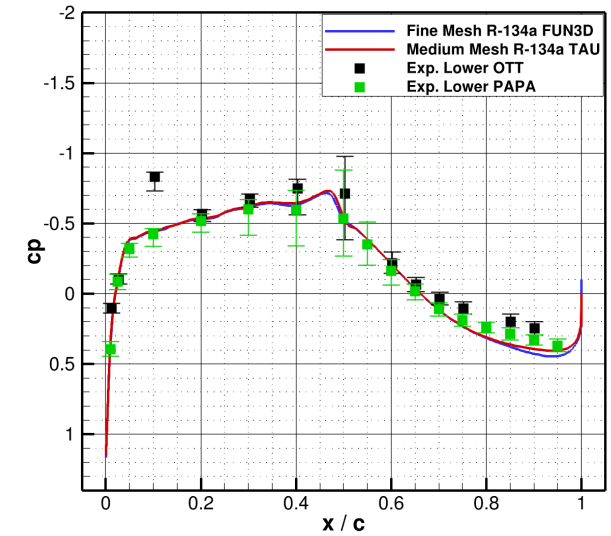
BSCW Mach = 0.8, AoA = -1 deg, Q = 169 psf
60% Span Station



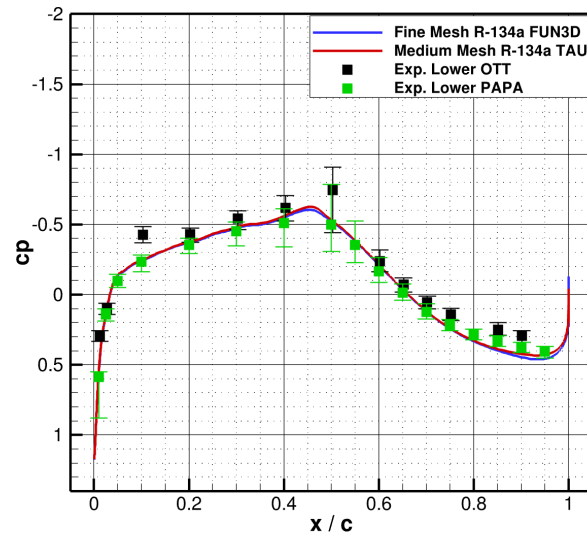
BSCW Mach = 0.8, AoA = 0 deg, Q = 169 psf
60% Span Station



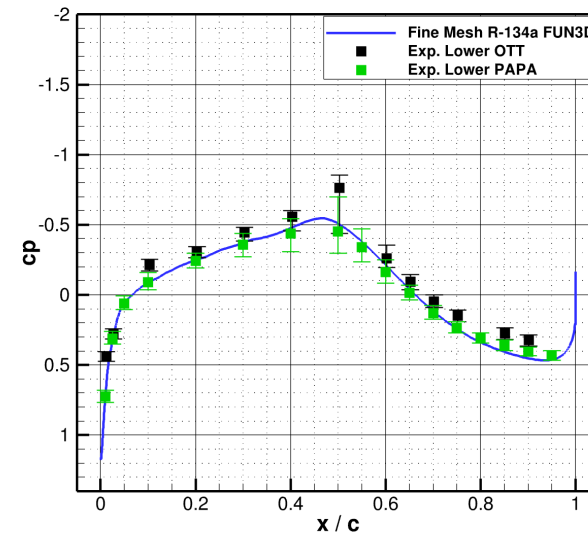
BSCW Mach = 0.8, AoA = 1 deg, Q = 169 psf
60% Span Station



BSCW Mach = 0.8, AoA = 3 deg, Q = 169 psf
60% Span Station



BSCW Mach = 0.8, AoA = 5 deg, Q = 169 psf
60% Span Station



Conclusions



- Mandatory
 - Flutter prediction at Mach 0.80 and angle-of-attack sweep: $0^{\circ} - 6^{\circ}$
- Optional
 - Flutter prediction at Mach 0.78, 0.76, 0.74 and angle-of-attack 3°
- **We use PAPA data (rigidized and flutter) for AePW-4 !!!**
- **Next BSCW experimental data (spring/summer 2025) must match existing PAPA data.**

June 13 slides



- An open and impartial forum to assess and evaluate the current state-of-the-art and state-of-the-practice in computational aeroelastic modeling
 - How effective are current solvers at predicting aeroelastic physics critical to aircraft analysis and design?
 - How can we understand the reasons for why our solvers may fail?
 - Can we establish best-practices for using aeroelastic solvers?
 - Can we establish uncertainty bounds for computational results?
 - Can we specify requirements on future validation experiments?
- What computational and experimental areas of research need further development?

Organizing Committee

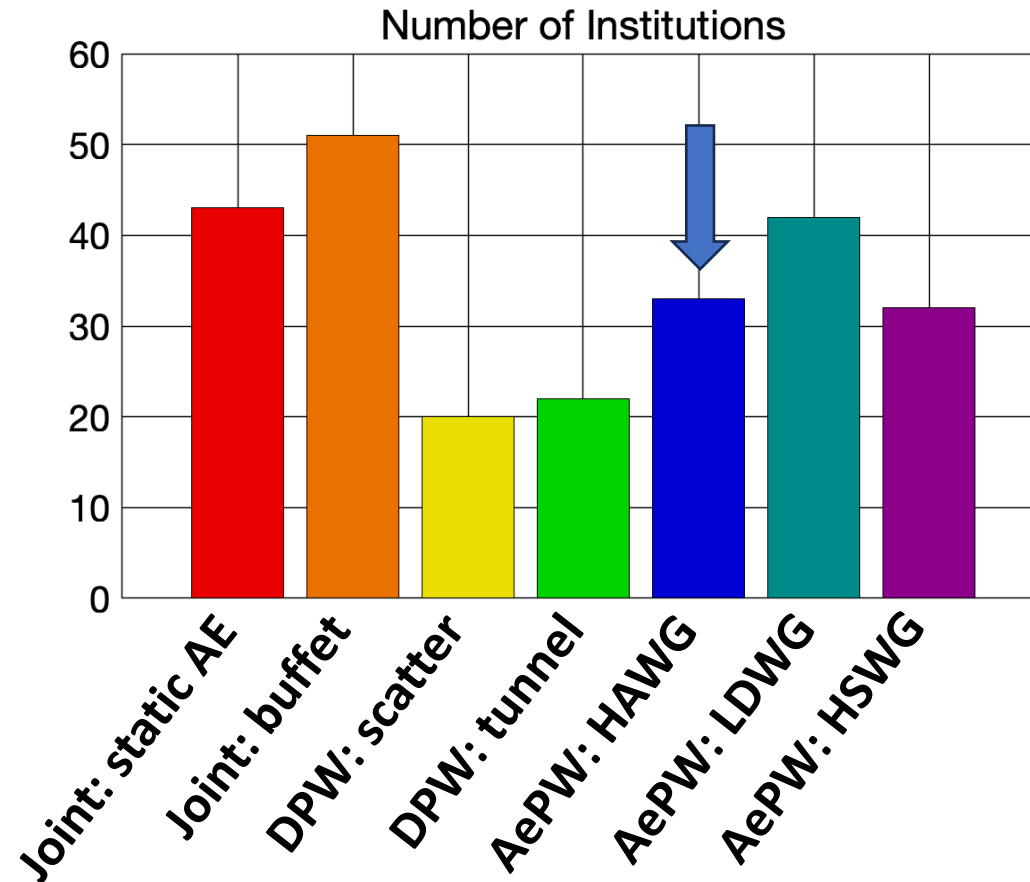


- Kirk Brouwer, AFRL (High-Speed WG)
- Carlos Cesnik, University of Michigan
- Pawel Chwalowski, NASA LaRC (High-Angle WG)
- Adam Jirasek, USAFA
- Jeff Ouellette, NASA LaRC
- Rafael Palacios, Imperial College London (High-Deformation WG)
- Daniella Raveh, Technion
- Markus Ritter, DLR
- Walt Silva, NASA LaRC
- Bret Stanford, NASA LaRC (AePW-4)

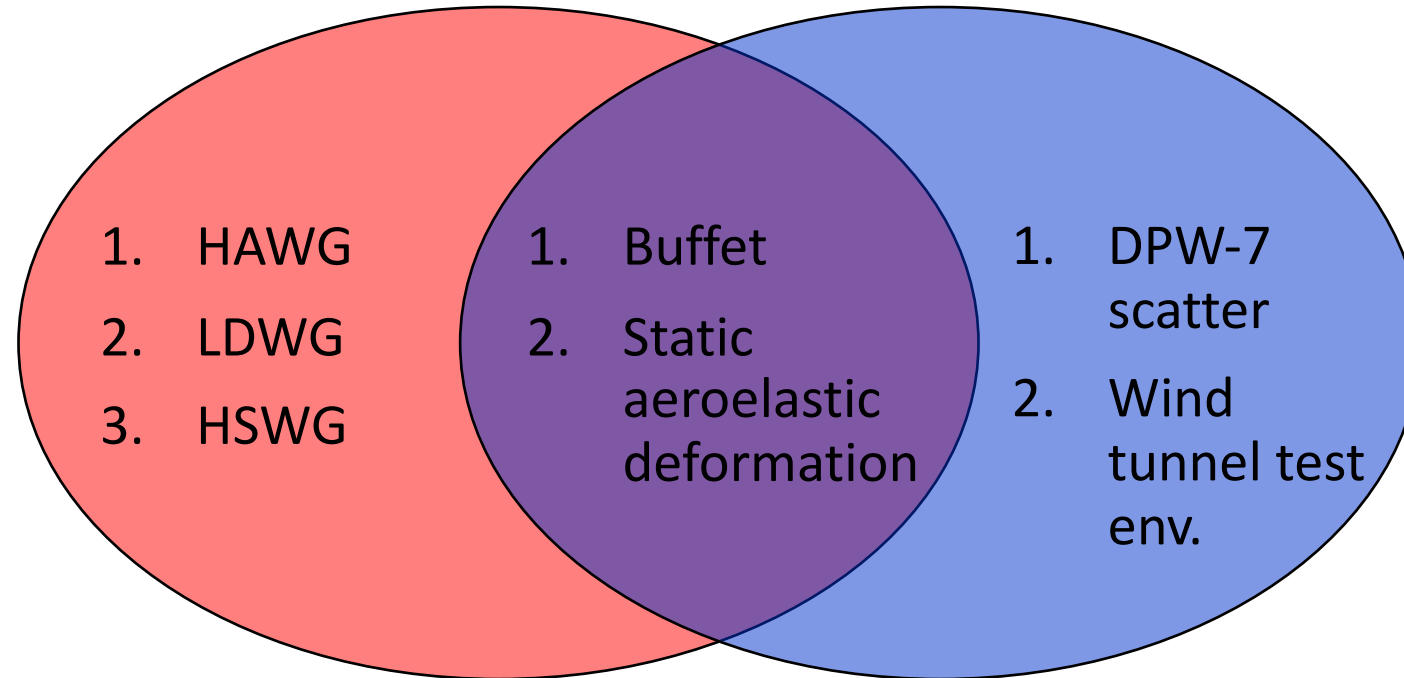
Transition to AePW-4; Joint Working Groups with DPW-8

<https://aiaa-dpw.larc.nasa.gov>

Joint workshop will take place at AIAA Aviation 2026

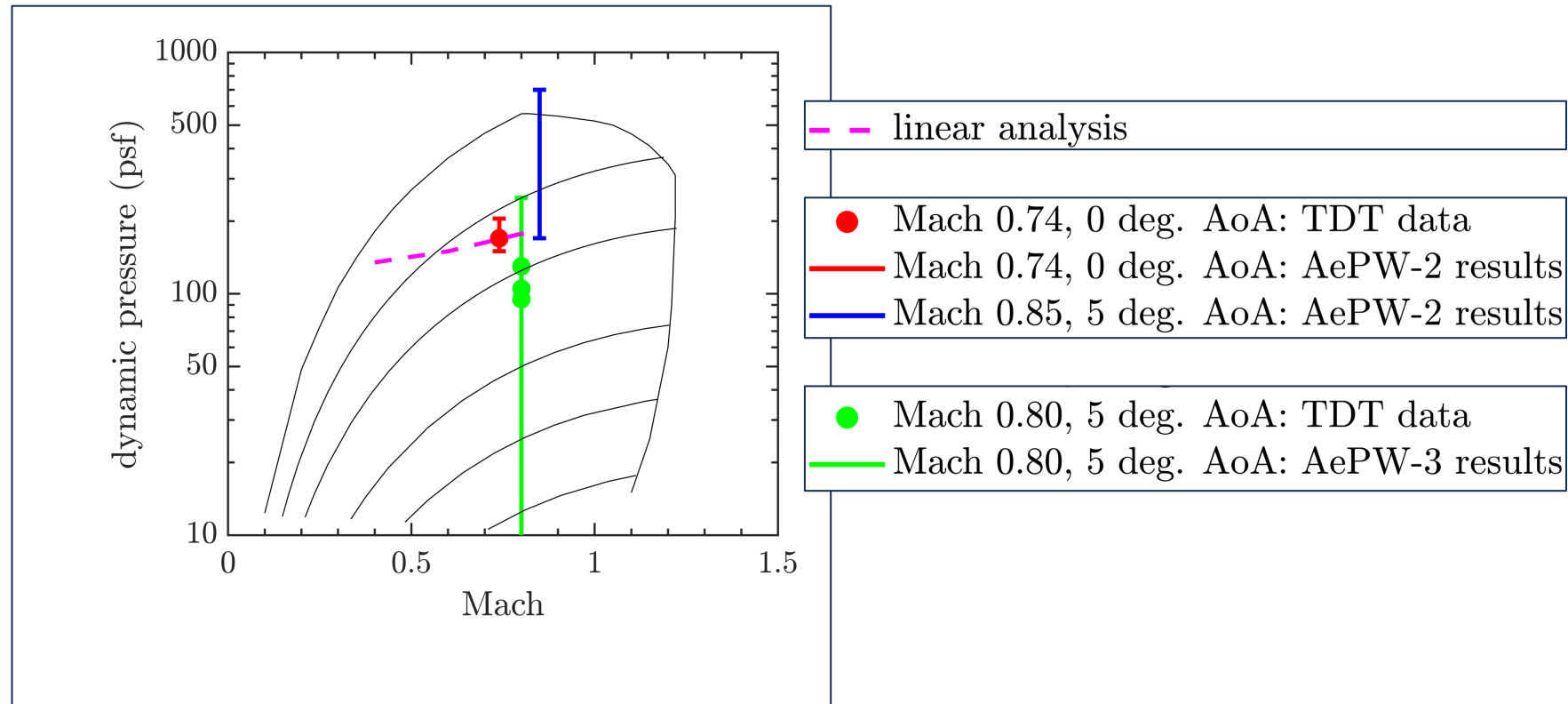


Venn Diagram of Working Groups



- AePW-1:
 - Steady-rigid and forced-oscillation cases at Mach 0.85, AoA = 5° ✓
- AePW-2:
 - Forced-oscillation case at Mach 0.70, AoA = 3° ✓
 - Flutter prediction at Mach 0.74, AoA = 0° ✓
 - Unsteady-rigid, forced-oscillation, and flutter cases at Mach 0.85, 5° ✓ ✓ ✓
- AePW-3:
 - Flutter prediction at Mach 0.80, AoA = 5° ✓
 - Shock-buffet case at Mach 0.80, AoA = 5° ✓
 - AIAA Paper 2024-0417 and 2024-0418

AePW-3: What have we learned?



- Large spread in BSCW flutter predictions from AePW-3 (though not as bad as AePW-2)
- We need more experimental data: more flutter data points, and more on-and off-body flow data at each flutter point

Past Experimental Data



**EXPERIMENTAL UNSTEADY PRESSURES AT
FLUTTER ON THE SUPERCRITICAL WING
BENCHMARK MODEL**

AIAA-93-1592-CP

Bryan E. Dansberry, Michael H. Durham*, Robert M. Bennett**, José A. Rivera*, Walter A. Silva*, and Carol D. Wieseman*; Structural Dynamics Division, NASA Langley Research Center, Hampton, VA 23681-0001 and David L. Turnock*
Lockheed Engineering and Sciences Corporation

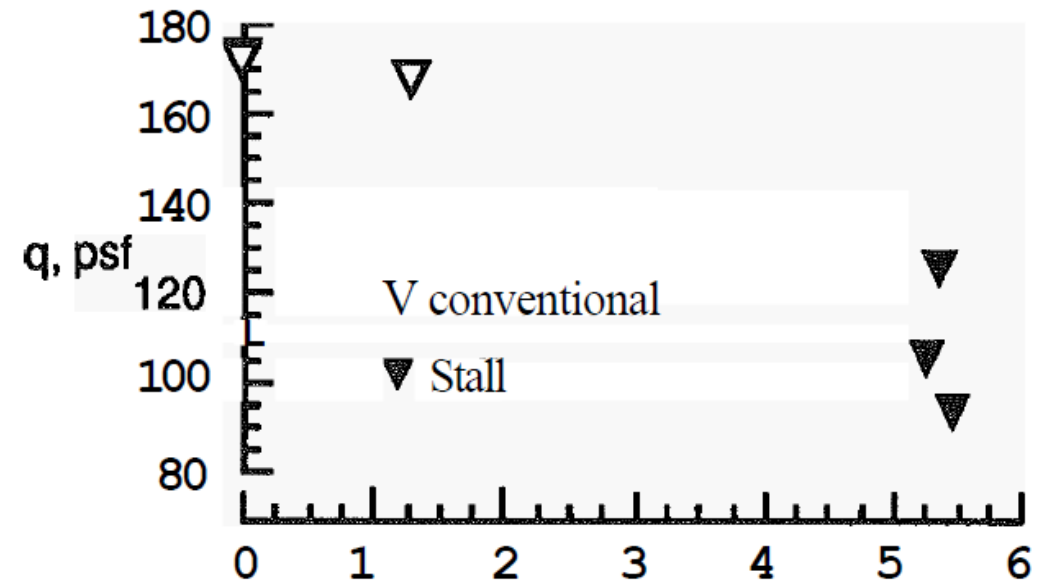


Figure 9. Stall flutter boundary in R-12 at $M = 0.80$.

Past Experimental Data



EXPERIMENTAL UNSTEADY PRESSURES AT
FLUTTER ON THE SUPERCRITICAL WING
BENCHMARK MODEL

AIAA-93-1592-CP

Bryan E. Dansberry, Michael H. Durham*, Robert M. Bennett**, José A. Rivera*, Walter A. Silva*, and Carol D. Wieseman*; Structural Dynamics Division, NASA Langley Research Center, Hampton, VA 23681-0001 and David L. Turnock*
Lockheed Engineering and Sciences Corporation

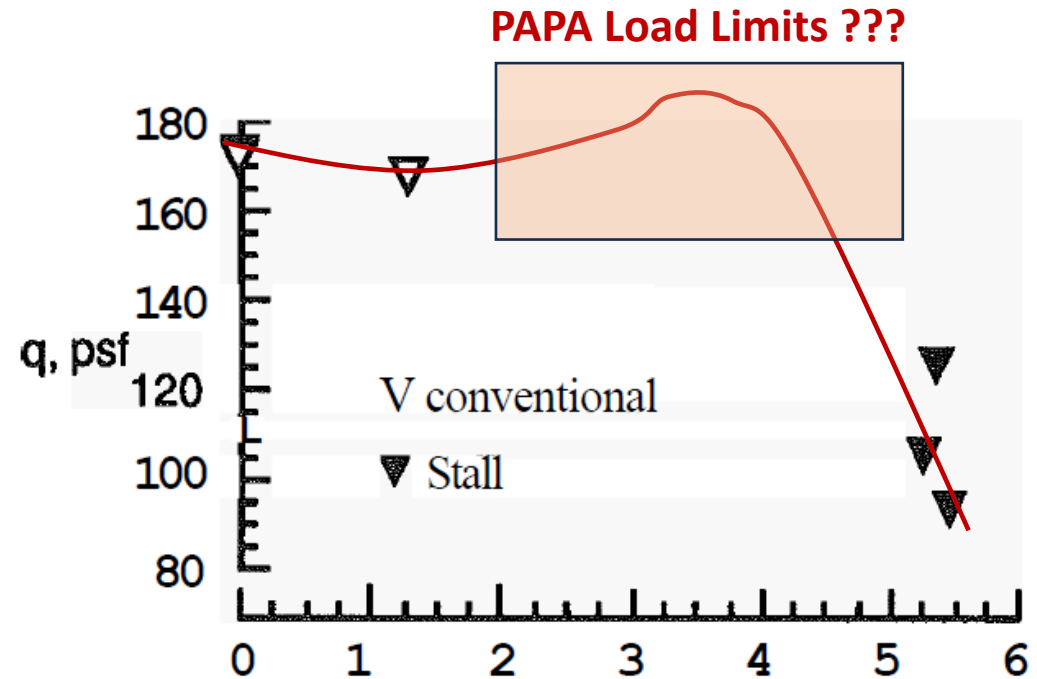


Figure 9. Stall flutter boundary in R-12 at $M = 0.80$.

Future Experiment: Spring 2025



- Re-examine factor of safety for PAPA load limits
- Unsteady Pressure Sensitive Paint
- Flutter Stopper
- Two rows of pressure sensors + several on splitter plate
- PIV
- Flutter and buffet data at Mach, Q, AoA range

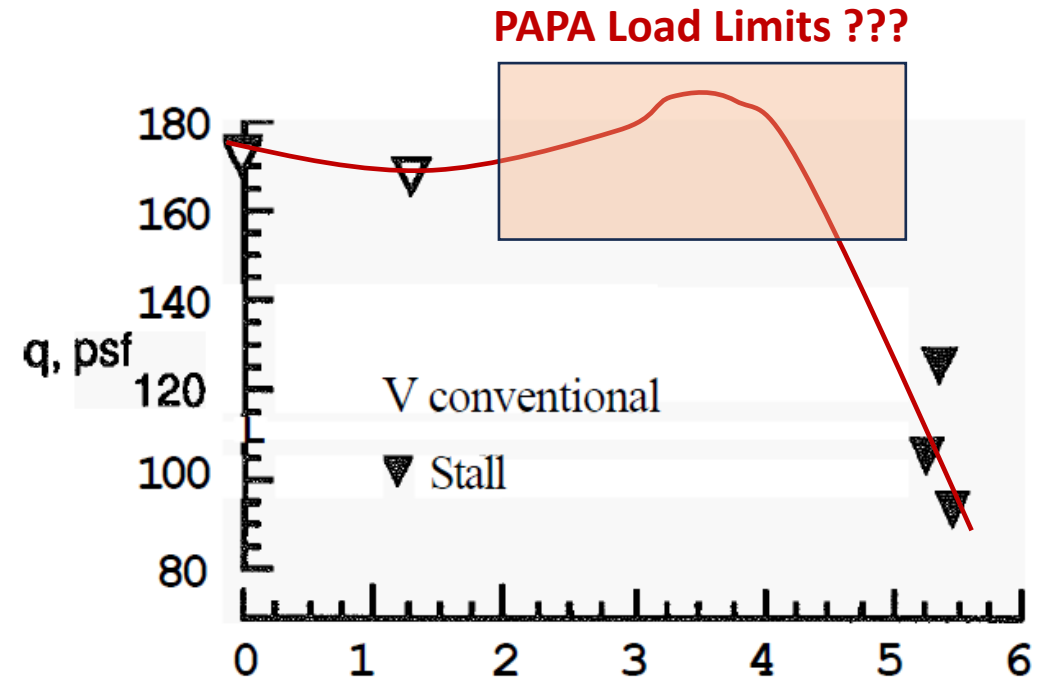


Figure 9. Stall flutter boundary in R-12 at $M = 0.80$.

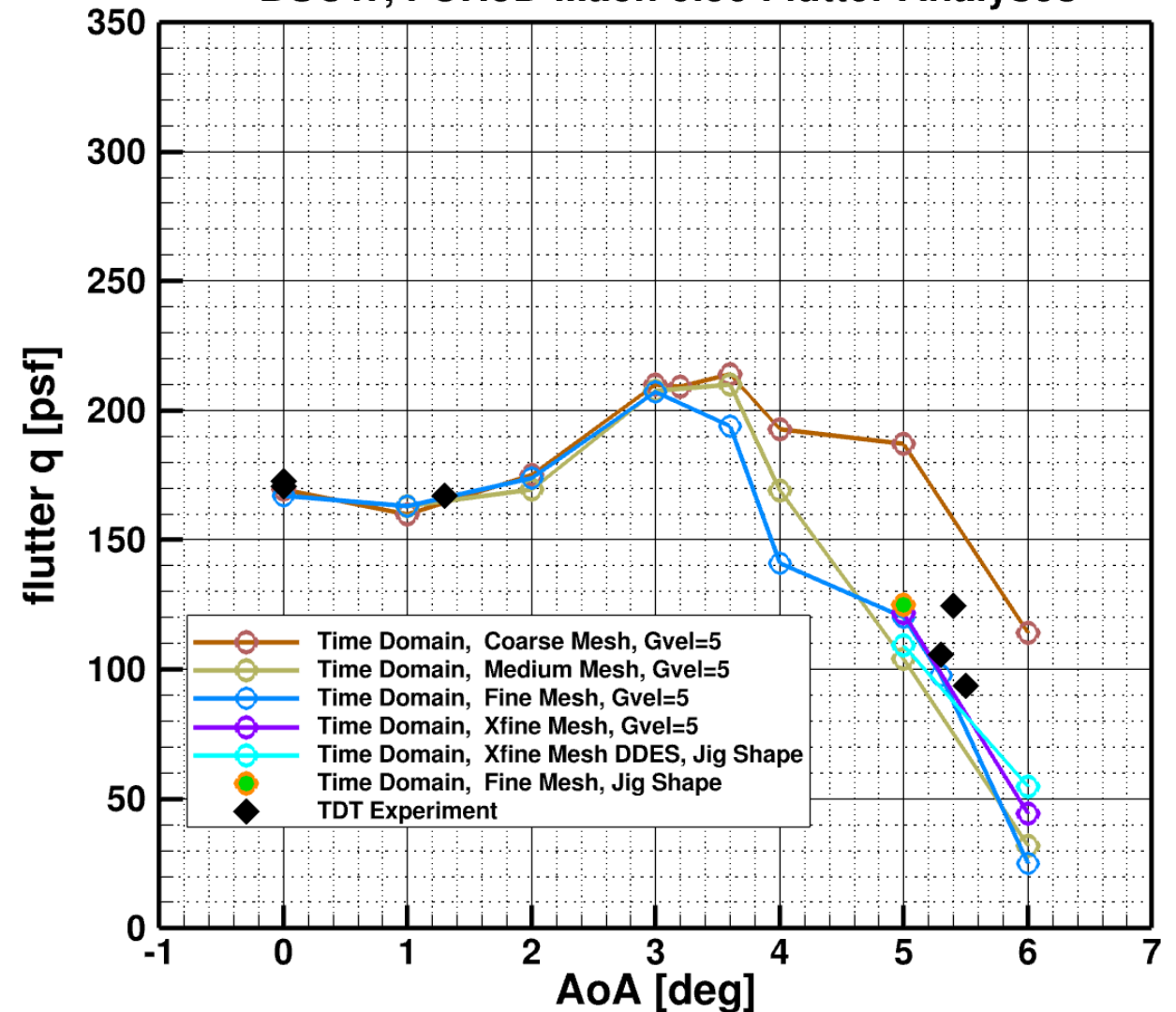
Current Computational Effort w/FUN3D

...trying to cover different methods...



- FUN3D URANS time domain analysis:
Rigid steady → Static aeroelastic →
Dynamic aeroelastic (with initial excitation using Gvel=5)
- Working on:
Rigid steady → Dynamic aeroelastic (Jig shape)
- Working on:
Scale-resolving DDES FUN3D time domain analysis:
Rigid steady → Static aeroelastic →
Dynamic aeroelastic (with initial excitation using Gvel)
- Working on:
Adding URANS solutions for Xfine Mesh

BSCW, FUN3D Mach 0.80 Flutter Analyses



Current Computational Effort w/FUN3D

...trying to cover different methods...



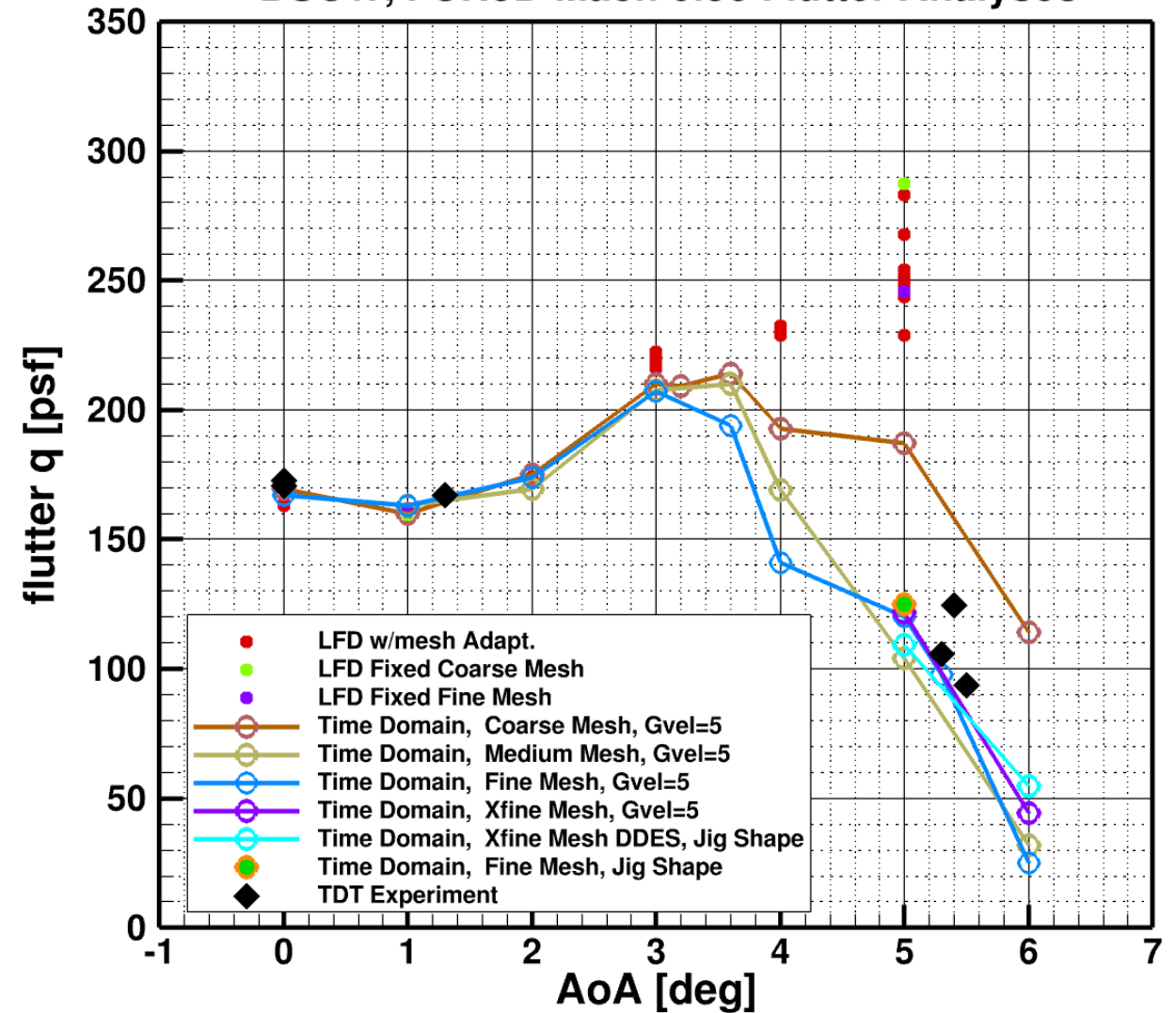
- FUN3D Linearized Frequency Domain (LFD):
Rigid steady → Static aeroelastic → LFD

LFD + Mesh Adaptation

- Working on:
Adding angle-of-attack sweeps

- ROM

BSCW, FUN3D Mach 0.80 Flutter Analyses

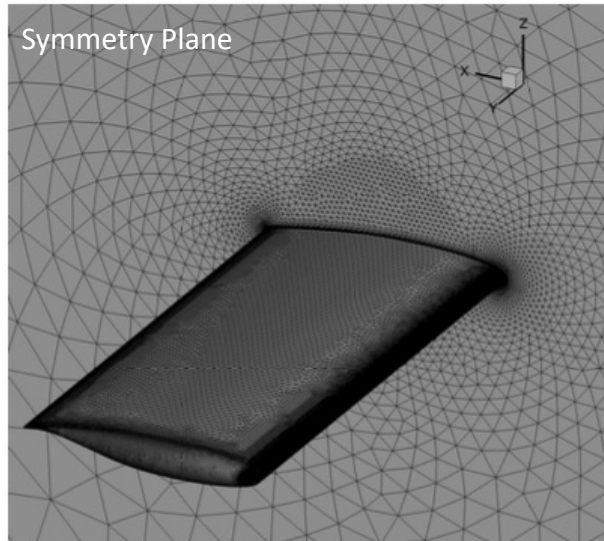


Schedule/Timeline/Logistics

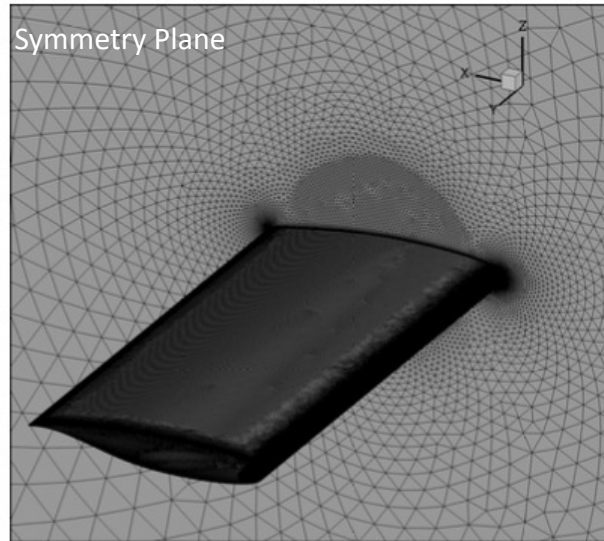


- Monthly meetings on second Thursday of each month at 10 am EDT
- IFASD 2024: 17 – 21 June 2024, The Hague - Bret Stanford
- AIAA Aviation 2024: Las Vegas, NV - Bret Stanford
- AIAA SciTech 2025: Orlando, FL (?)
- Spring 2025: New BSCW Experiment (Data release ?)
-
-
- AIAA Aviation 2026: DPW-8 and AePW-4 Workshop

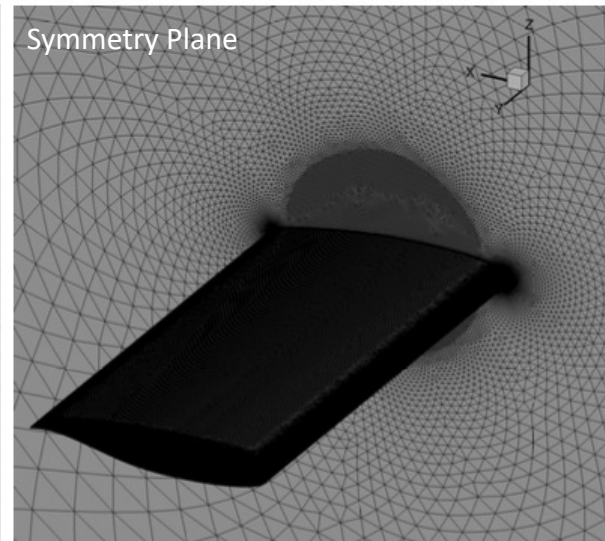
- On AePW-2 website: <https://nescacademy.nasa.gov/workshops/AePW2/public/> under Analysts Information you can download BSCW iges file. Gridding guidelines adopted from the DPW are also listed.
- Note that the iges file consists of BSCW wing mounted on a splitter plate. But...
- For AePW-1, AePW-2, and AePW-3, we assumed wing-only that is attached to a plane of symmetry.
- Several grids are also available for download. But do we need to build and provide new grids?
- BSCW structural model is described, and NASTRAN files are available.



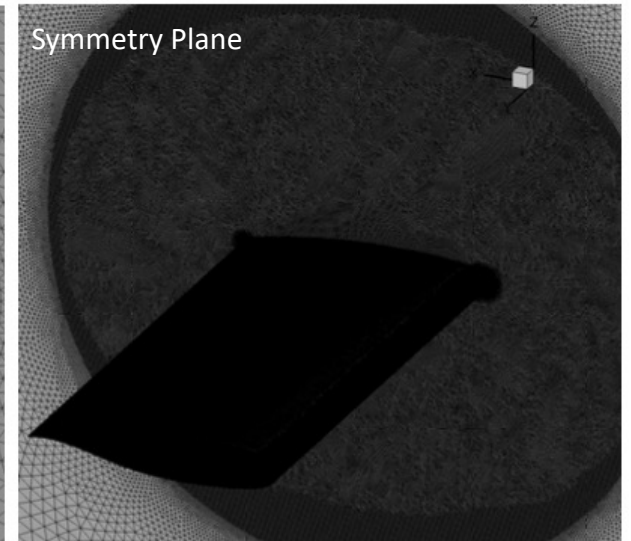
(a) Coarse grid, 3M nodes.



(b) Medium grid, 9M nodes.



(c) Fine grid, 27M nodes.



(d) Xfine grid, 99M nodes.

Node centered.... 'nc'
Cell centered.... 'cc'



AePW-3 Summary Paper, <https://doi.org/10.2514/6.2024-0418>

Table 2 BSCW flow conditions: Mach 0.8 with range of dynamic pressure (q); chord Reynolds number (Re_c); Reynolds number per foot (Re); velocity (V); speed of sound (a); static temperature, (T_{static}); density (ρ); ratio of specific heat (γ); viscosity (μ); Prandtl number (Pr); total pressure (H); and static pressure (P).

Mach	0.799	0.8	0.8	0.8	0.8	0.8	0.8	0.8	0.8	0.8	0.8	0.801	0.801
q [psf]	10.02	25.00	35.00	50.00	75.00	100.00	134.00	143.00	152.00	168.80	200.00	225.00	250.00
Re_c	237461	592224	829213	1184801	1777732	2371336	3178880	3392751	3606668	4006103	4748658	5343835	5939368
Re [1/ft]	178096	444168	621910	888601	1333299	1778502	2384160	2544563	2705001	3004577	3561493	4007876	4454526
V [ft/s]	440.45	440.63	440.59	440.51	440.39	440.21	440.05	440.00	439.96	439.88	439.70	439.58	439.46
a [ft/s]	551.08	550.94	550.85	550.71	550.48	550.25	549.94	549.86	549.78	549.62	549.34	549.11	548.88
T_{static} [$^{\circ}F$]	80.87	80.83	80.83	80.82	80.81	80.80	80.78	80.77	80.77	80.76	80.74	80.73	80.71
ρ [slug/ft ³]	0.000103	0.000258	0.000361	0.000515	0.000774	0.001032	0.001384	0.001477	0.001571	0.001745	0.002069	0.002329	0.002589
γ	1.1121	1.1122	1.1123	1.1124	1.1126	1.1128	1.1131	1.1131	1.1132	1.1133	1.1136	1.1138	1.1139
μ [lb-sec/ft ²]	2.555e-07	2.555e-07	2.555e-07	2.555e-07	2.555e-07	2.555e-07	2.554e-07	2.554e-07	2.554e-07	2.554e-07	2.554e-07	2.554e-07	2.554e-07
Pr	0.68394	0.68404	0.68410	0.68419	0.68435	0.68450	0.68471	0.68477	0.68483	0.68493	0.68513	0.68528	0.68544
H [psf]	40.00	99.72	139.61	199.45	299.18	399.00	534.69	570.61	606.53	673.59	798.21	898.01	997.83
P [psf]	28.21	70.32	98.45	140.64	210.97	281.37	377.05	402.38	427.71	475.00	562.87	633.25	703.64



Mach 0.74

Mach	0.74	0.74	0.74	0.74	0.74	0.74	0.74	0.74
q [psf]	50.00	75.00	100.00	134.00	143.00	152.00	168.80	200.00
Re_c	1275964	1914959	2554246	3423935	3654400	3884927	4315413	5115471
Re [1/ft]	956973	1436219	1915684	2567951	2740800	2913695	3236560	3836603
V [ft/s]	407.58	407.37	407.23	407.09	407.04	406.99	406.89	406.71
a [ft/s]	550.82	550.56	550.30	549.93	549.84	549.74	549.56	549.23
T_{static} [$^{\circ}F$]	83.60	83.59	83.58	83.55	83.55	83.54	83.54	83.52
ρ [slug/ft ³]	0.000602	0.000904	0.001206	0.001617	0.001726	0.001836	0.002039	0.002418
γ	1.1116	1.1119	1.1121	1.1124	1.1125	1.1125	1.1127	1.1130
μ [lb-sec/ft ²]	2.564E-07	2.564E-07	2.564E-07	2.564E-07	2.564E-07	2.564E-07	2.564E-07	2.563E-07
Pr	0.68325	0.68343	0.68360	0.68385	0.68391	0.68398	0.68410	0.68432
H [psf]	221.92	332.99	444.03	594.95	634.93	674.92	749.56	888.22
P [psf]	164.50	246.83	329.14	441.01	470.65	500.29	555.62	658.40



Mach 0.76

Mach	0.76	0.76	0.76	0.76	0.76	0.76	0.76	0.76
q [psf]	50.00	75.00	100.00	134.00	143.00	152.00	168.80	200.00
Re_c	1245425	1868520	2492233	3341185	3566044	3790959	4210646	4991103
Re [1/ft]	934069	1401390	1869175	2505889	2674533	2843219	3157984	3743327
V [ft/s]	418.22	418.15	418.01	417.82	417.78	417.73	417.67	417.50
a [ft/s]	550.43	550.18	549.93	549.58	549.49	549.40	549.23	548.92
T_{static} [$^{\circ}F$]	82.72	82.70	82.69	82.67	82.67	82.66	82.65	82.63
ρ [slug/ft ³]	0.000572	0.000858	0.001145	0.001535	0.001639	0.001742	0.001936	0.002295
γ	1.1118	1.1120	1.1122	1.1125	1.1125	1.1126	1.1128	1.1130
μ [lb-sec/ft ²]	2.560E-07	2.560E-07	2.560E-07	2.560E-07	2.560E-07	2.560E-07	2.560E-07	2.559E-07
Pr	0.68360	0.68377	0.68394	0.68417	0.68423	0.68430	0.68441	0.68463
H [psf]	213.86	320.74	427.68	573.16	611.67	650.19	722.01	855.54
P [psf]	155.96	233.91	311.91	418.00	446.09	474.18	526.56	623.94



Mach 0.78

Mach	0.78	0.78	0.78	0.78	0.78	0.78	0.78	0.78
q [psf]	50.00	75.00	100.00	134.00	143.00	152.00	168.80	200.00
Re_c	1216355	1824869	2433950	3262935	3482495	3702106	4112185	4874236
Re [1/ft]	912266	1368652	1825462	2447201	2611871	2776579	3084139	3655677
V [ft/s]	428.90	428.83	428.70	428.53	428.48	428.43	428.35	428.19
a [ft/s]	550.03	549.79	549.55	549.22	549.13	549.05	548.88	548.58
T_{static} [$^{\circ}F$]	81.82	81.80	81.79	81.77	81.76	81.76	81.75	81.73
ρ [slug/ft ³]	0.000544	0.000816	0.001088	0.001460	0.001558	0.001656	0.001840	0.002182
γ	1.1119	1.1121	1.1123	1.1125	1.1126	1.1127	1.1128	1.1131
μ [lb-sec/ft ²]	2.556E-07	2.556E-07	2.556E-07	2.556E-07	2.556E-07	2.556E-07	2.555E-07	2.555E-07
Pr	0.68396	0.68413	0.68429	0.68451	0.68457	0.68463	0.68474	0.68495
H [psf]	206.41	309.56	412.78	553.16	590.33	627.50	696.88	825.74
P [psf]	148.06	222.05	296.08	396.78	423.44	450.10	499.87	592.30

AePW-4 High-Angle Working Group Meeting



June 13, 2024
Pawel Chwalowski
Pawel.Chwalowski@nasa.gov